

# Research on the mechanism of dynamic avalanche induced by IGBT short circuit and its influencing factors

Yuting Liu

Agricultural water conservancy project, Hohai University, 210024, China  
liuyt6660901@163.com

## Abstract:

The insulated gate bipolar transistor (IGBT) is currently the most important power electronic device. It has a simple drive circuit, high operating frequency, and stable temperature. Through structural optimization and the development of new materials, its voltage and power levels have gradually increased. First, a four-unit parallel device model was established, and the electric-thermal coupling numerical simulation method was used to simulate the current, electric field, hole concentration, temperature distribution, impact ionization rate and other parameters during the dynamic avalanche process of Type II IGBT, revealing the conditions under short-circuit conditions. dynamic avalanche mechanism. On this basis, different structural parameters were compared and analyzed.

**Keywords:** IGBT short circuit, dynamic avalanche, influencing factors

## 1 Introduction

A common fault form of IGBT is short circuit, which means that the device operates in an unexpected state or with extremely small bus parasitic inductance, causing its junction temperature to rise rapidly. If it is not disconnected in time, it will cause serious consequences. Therefore, it is necessary to control the short-circuit time of IGBT and try to enhance its short-circuit tolerance [1]. In addition, in the event of a short circuit, IGBT may also suffer additional transient failures, leading to device failure. Currently, in order to further improve their performance, mainstream semiconductor manufacturing companies adopt ultra-thin structures. However, this results in a decrease in their heat capacity and more obvious current concentration during short-circuit shutdown, which in turn leads to a decrease in their short-circuit capability. This poses higher requirements for the short-circuit reliability and durability of IGBT, and it is of great significance to conduct in-depth research on its short-circuit mechanism and characteristics.

## 2 The mechanism of dynamic avalanche induced by short circuit and its influencing factors

### 2.1 Research on dynamic avalanche mechanism during secondary short circuit

Using a 4-unit parallel structure, the dynamic avalanche characteristics of IGBT during short circuit were studied

and electrothermal coupling simulation was performed.

#### 2.1.1 Mechanism analysis of dynamic avalanche when short circuit II occurs

During a secondary short circuit, both the voltage and current increase rapidly, and a large VC/SC (on) will cause a dynamic avalanche. Figure 4-1 shows the voltage-current curve during the first short circuit, as well as the vertical field strength and void concentration distribution at each moment when  $X=20$  microns. When a short circuit occurs, the device enters the conducting state, and there are a large number of carriers in the n-type drift region, which rise rapidly after the short circuit. At  $t_1$ , because the voltage is still saturated, the electric field is very weak, and the space at the J2 junction is first widened, and the electric field gradually becomes larger[2]. At  $t_2$ , the current reaches its maximum value, and the voltage is also in a rapidly rising stage. The electric field intensity at this stage increases significantly and expands toward the collecting electrode. Under the action of the electric field, plasma is extracted and the holes move toward the collecting electrode. The electrons flow to one side of the emitter region, while other electrons flow toward the collector region, forming an S shape. At time  $t_3$ , the electric field has expanded to the nFS layer, and the voltage at time  $t_3$  is 3377 V, which is much lower than the blocking voltage. However, due to the carrier-modulated electric field, the peak electric field  $E_{pn}$  of the J2 junction is very large, and currently  $E_{pn}$  has reached  $2.3 \times 10^5$  V/cm, exceed-

ing the threshold, and the device experienced a dynamic avalanche phenomenon. During this process, with the generation of avalanche carriers, the movement rate of the plasma interface gradually slows down, and the change in the electric field also decreases. As shown in Figure 1, the increase in voltage tends to be gentle. At time t4, the intensity of the avalanche further increases, and by that time,  $E_p$  has risen to  $2.7 \times 10^5$  V/cm.

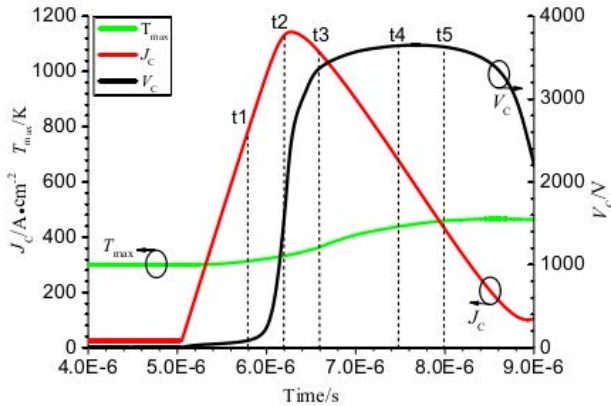


**Figure 1 Short circuit II turn-on current density and voltage curves**

Figure 2 depicts the collision ionization rate at different time points, while Figure 3 shows the ionization curve at an unspecified time point. At t1, due to the small electric field intensity, the impact ionization rate in the J\_2 base region is very low, so there will be no avalanche phenomenon. The results indicate that when the applied voltage and electric field intensity are both high, the impact ionization rate at the J2 junction also increases, and the electron current density below the p-base region increases. At t4, the impact ionization rate at the J2 junction reaches a very high peak, forming a large number of avalanche

carriers, and the electron flow below the p-base region also increases significantly, indicating that the dynamic avalanche has been very intense. [3] If you compare the collapsed electrons with the extracted electrons, then the plasma boundary will move slowly, the change in the electric field will become very small, and the voltage will basically not change at all. During the kinetic avalanche process, the junction temperature continues to increase. As the temperature rises, the avalanche-impact ionization rate decreases, the kinetic avalanche weakens, and the voltage decreases.

Therefore, when the short circuit starts again, a dynamic avalanche phenomenon will occur. During a kinetic avalanche, the high impact ionization rate of J\_2 will form more avalanche carriers, thereby increasing the hole current in the p-base region below the n-emitter region, thereby triggering the conduction of the thyristor switch. This causes the device to latch up and cause device failure[4].

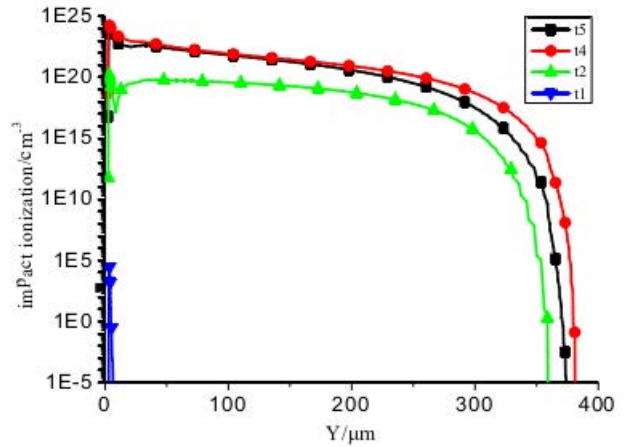


**Figure 2 Impact ionization rates at different times**

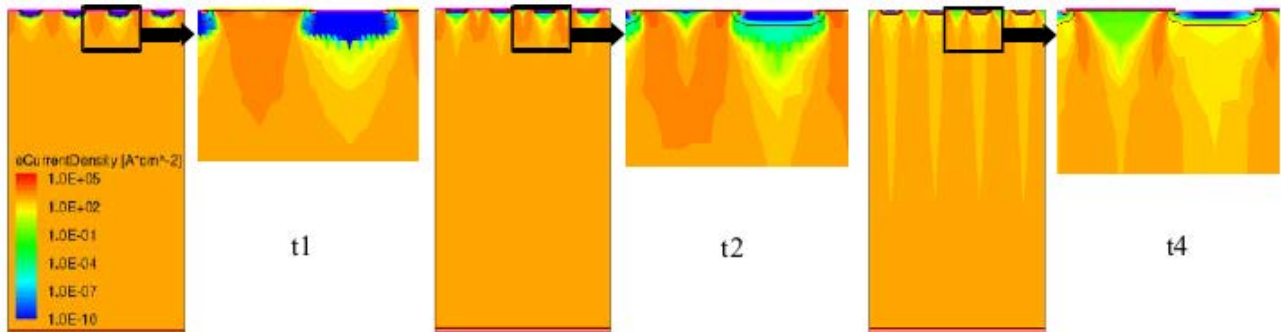


**Figure 3 Electron current density distribution diagram at t1, t2 and t4**

**2.1.2 Mechanism analysis of dynamic avalanche during short circuit II turn-off**

When the short circuit II is opened, the induced voltage  $V/SC$  (off) across the large inductance is very large, and a

dynamic avalanche phenomenon will also occur. Figure 4 shows the disconnection process in short circuit II mode. It can be seen that at t1, the gate becomes a negative voltage, but the device does not disconnect, clamping occurs, and the current decreases slowly, remaining closed for

longer. Figure 5 shows the electron concentration distribution and impact ionization rate curve at each time point when  $x=40$  microns. It can be seen from the figure that the charge density and impact ionization rate at the J2 junction are very small at time  $t_0$ . When the voltage increases, the impact ionization rate and electron concentration at the J2 junction increase significantly, and, accompanied by the avalanche effect, the charge density at the J2 junction increases to  $1.7 \times 10^{14} \text{ cm}^{-3}$ . At time  $t_4$ , the impact ionization rate decreases, the charge density at the J2 junction also decreases, and the kinetic collapse intensity diminishes. At time point  $t_7$ , the residual carrier concentration is basically extracted and the device turns off.

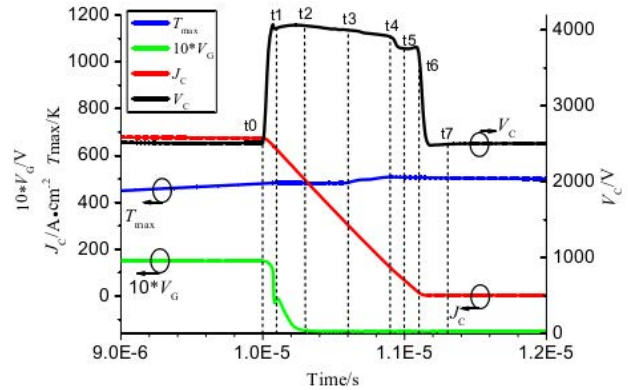
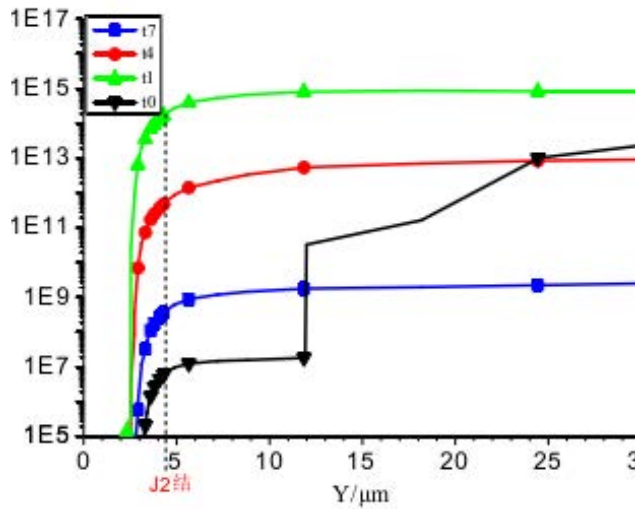
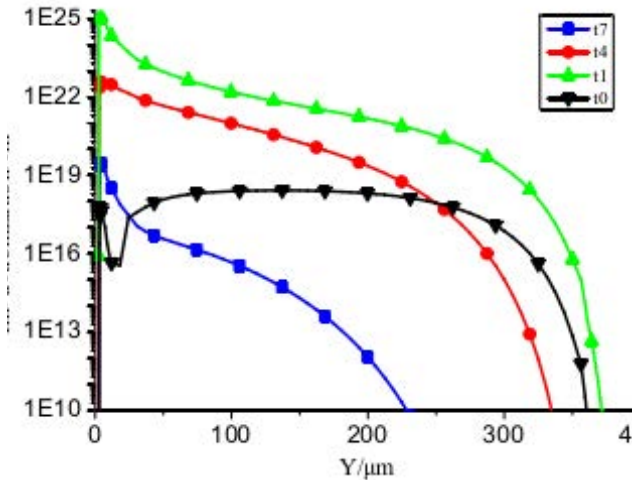


Figure 4 Short circuit II turn-off current and voltage curves



(a) Electron density distribution diagram



(b) Impact ionization rate

Figure 5 Electron density distribution diagram and impact ionization rate at different times

Figure 6 is the current density curve at the corresponding time point. The MOS channel disappears at  $t_1$ , so the current flows directly from the p base region to the emitter region. The currents on the four cells are still relatively consistent at  $t_1$ . During this process, two current accumulation areas (i.e., current strips) will be generated in the battery cell cavity, and the current density of one strip will

increase significantly[5]. At time  $t_5$ , the current filament moves toward the second cell to the right, and the current density gradually decreases. During this process, as the plasma continues to be extracted, the current lines gradually decrease until  $t_6$ , when the current lines disappear and the device gradually turns off.

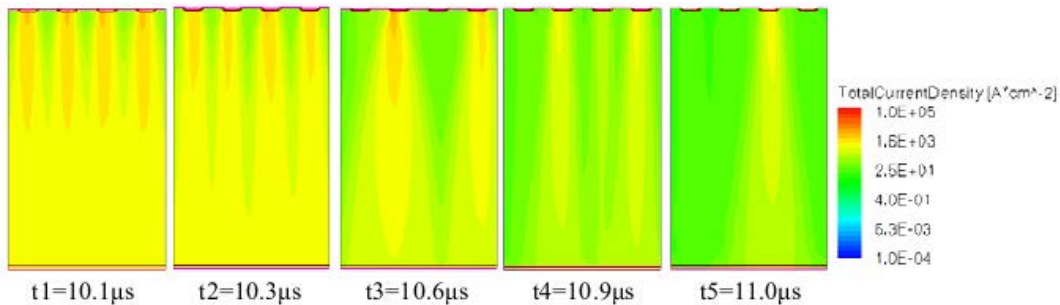


Figure 6 Current density distribution diagram at different times

Figure 7 shows the distribution of longitudinal field strength and hole concentration at each moment when  $x=40$  microns. Time  $t_0$  is the short-circuit stable state, which indicates that the carrier concentration in the n-drift region compensates for the background doping, so the effective charge density  $N_{eff}$  is close to 0. At time  $t_1$ , when the current decreases, the voltage at the large inductor quickly rises to 4028 V, and the current decreases to 625 A/cm<sup>2</sup>. Although the collector-emitter voltage at this time is lower than the blocking voltage, when it is turned off due to a short circuit, There are a large number of carriers in the device. When the voltage increases, the charges flow to the collector side and the holes flow to the emitter area, causing the electric field gradient to increase and present an S-shaped distribution. When the voltage has not yet reached the cut-off voltage, the peak electric field  $E_{pn}$  has reached the critical breakdown field, and an avalanche will occur at the J2 junction. Therefore, at  $t_1$ , the number of carriers on the emitter side increases significantly, and the kinetic avalanche effect causes the carrier pumping rate to decrease. Slowly, the current decay slows down[6]. At time  $t_4$ , the residual carrier concentration gradually decreases, therefore, the electric field becomes steeper and  $E_{n+}$  becomes smaller and smaller. During the avalanche, the injection into the side hole of the current collector will cause the plasma at the current collector end to continuously increase, causing the electric field at the current collector end to be squeezed, resulting in a “clamping” phenomenon, thereby prolonging the Closing time. At time  $t_7$ , the device is disconnected and the voltage returns to the bus voltage. At this time, the magnetic field is distributed in a triangle, but there is still residual plasma in the n-type buffer layer, which indicates that leakage still exists during the short-circuit turn-off process. Therefore, when the short circuit is opened, a dynamic avalanche will occur when the voltage on the collector is below the cut-off voltage. This violent dynamic avalanche will cause the voltage of the collector to be clamped, resulting in the formation of current filaments.

Figure 8 is the temperature curve at the off time  $t_1$  and time  $t_4$  in the short circuit II mode. In a short period of time, the junction temperature rises rapidly. At  $t_1$ , the maximum temperature rise of the device is 484 K, and a large number of current filaments appear in this area, and in the area near the filaments, the temperature of the device It rises faster. At  $t_4$ , the maximum temperature of the device has reached 510 K, located at the position of the secondary current wire on the left. When the temperature increases, the kinetic collapse-collision ionization rate decreases, the plasma interface moves to the side of the current collector, the J2 junction peak field decreases, and

the current filament weakens, but the current intensity decreases significantly.

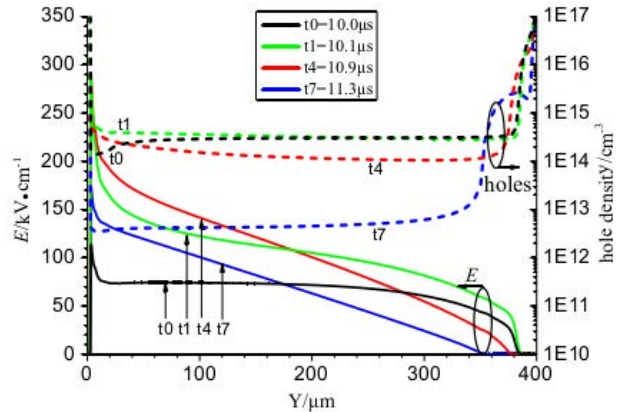


Figure 7 Electric field and hole density distribution diagram at different times

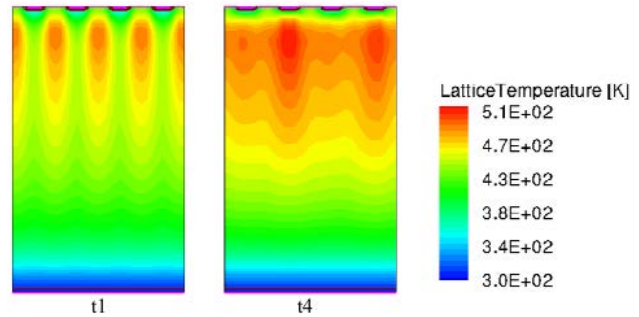


Figure 8 Temperature distribution inside the device at  $t_1$  and  $t_4$

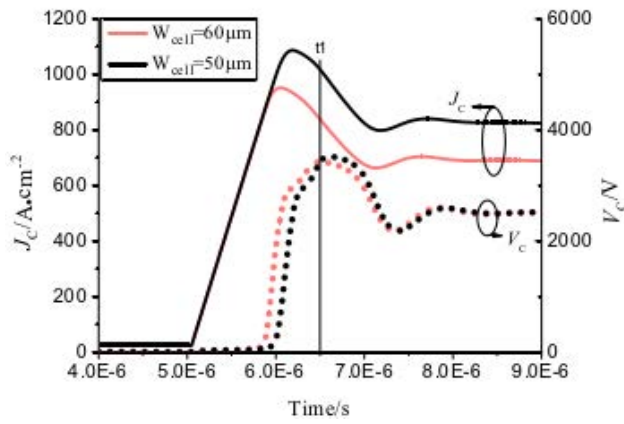
During short-circuit turn-off, due to the existence of parasitic inductance, an extremely high induced voltage peak occurs, which is prone to dynamic avalanche phenomena; under the action of short-circuit current, due to changes in carrier concentration, the J2 junction peak field Dynamic avalanche phenomena below blocking voltage. Strong dynamic collapse will form current filaments in the p-base region, causing the device temperature to rise significantly. However, in actual engineering, under non-uniform conditions, current filaments can easily appear, and the local temperature of the device will rise, resulting in The device is overheated.

## 2 Effect of structural parameters on dynamic avalanche during short circuit process

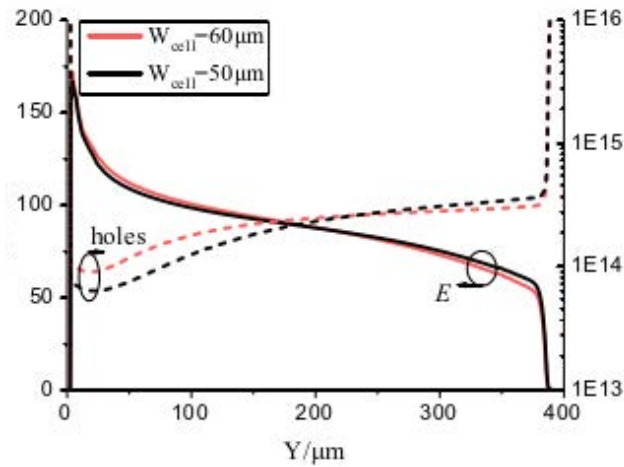
### 2.1 Cell size

The size of the unit body will significantly affect the short-circuit current of the battery, which in turn affects the carrier concentration in the battery, and thus indirectly affects the field strength distribution of the battery. Figure

9 (a) is the waveform when a short circuit with different cell sizes occurs in short circuit II mode. It can be seen from the chart that the smaller the size of the unit, the higher the short-circuit current density, and the greater the peak voltage of the short-circuit voltage. Figure 9(b) shows the longitudinal electric field and the corresponding hole concentration distribution under the maximum electric field at t1[7]. It can be seen that as the cell size increases, more holes accumulate in the n-drift region, while in the emission The hole concentration in the polar region also increases, but because the difference between the electric field gradient and  $E_{pn}$  is very small, the cell size has little impact on the dynamic avalanche during the short circuit process.



(a) Current and voltage curves when short circuit II occurs

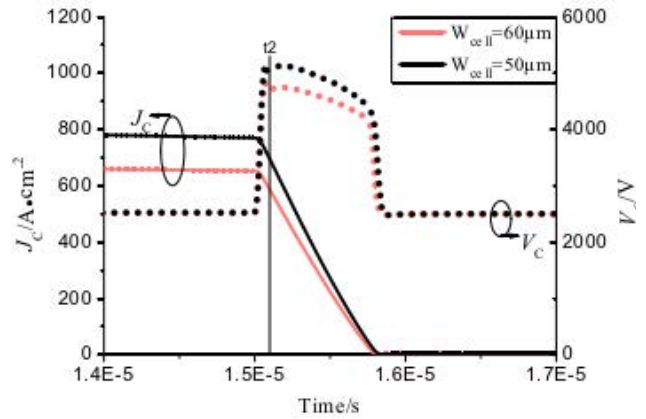


(b) Electric field and hole density distribution diagram at time t1

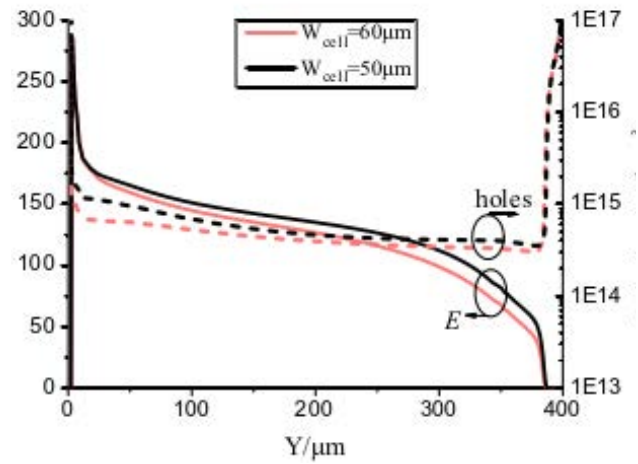
**Figure 9 Short-circuit current and voltage curves under different cell sizes and electric field and hole density distribution at time t1**

Figure 10 shows the short-circuit opening waveforms under different unit sizes and the field strength distribution at time t2 in the second short-circuit mode at x=24 microns

at time t2. It can be seen from the chart that the smaller the size of the unit, the higher the short-circuit current density, and the higher the current drop rate during short-circuit turn-off, the greater the peak VC/SC (off) of the induced voltage. As shown in Figure 10 B, the smaller the cell unit size, the higher the current density in the same time,  $E_{pn}$  increases with more hole concentration, when the cell unit size is 50 microns and 60 microns,  $E_{pn}$  are  $2.96 \times 10^5$  V/cm and  $2.85 \times 10^5$  V/cm respectively.



(a) Short circuit II turn-off current and voltage curves



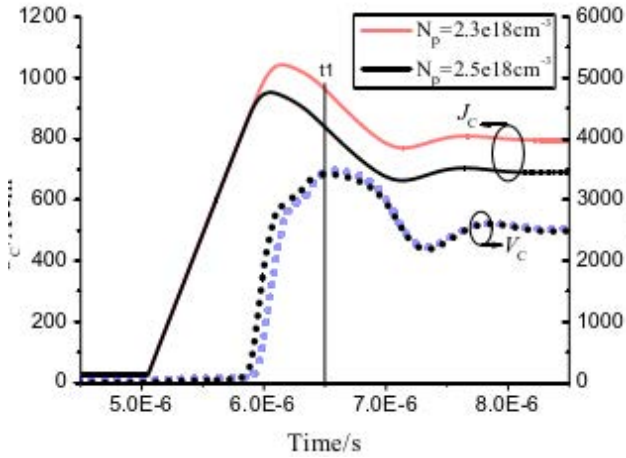
(b) Electric field and hole density distribution diagram at time t2

**Figure 10 Short-circuit II turn-off current, voltage curve and electric field and hole density distribution at time t2 under different cell sizes**

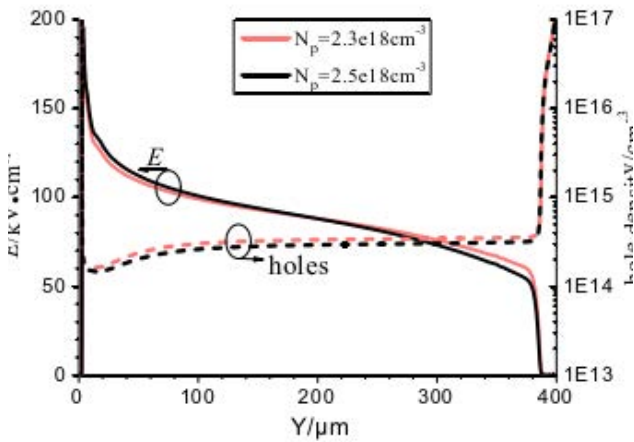
**2.2 p base region concentration**

Figure 11 shows the waveform of the short-circuit open circuit under different P base region concentrations in the second short-circuit mode, and the field intensity distribution under the maximum electric field at t1. As the p-base concentration decreases, the  $E_{pn}$  of t1 becomes lower.

In different p-base regions,  $E_p$  is  $1.95 \times 10^5$  V/cm in the range of  $2.5 \times 10^{18}$  cm<sup>-3</sup>, while in  $2.3 \times 10^{18}$  cm<sup>-3</sup>,  $E_p$  is  $1.89 \times 10^5$  V/cm. When  $N_p$  is small, avalanche holes passing through the P base region are more likely to form a latch-up phenomenon.



(a) Current and voltage curves when short circuit II occurs

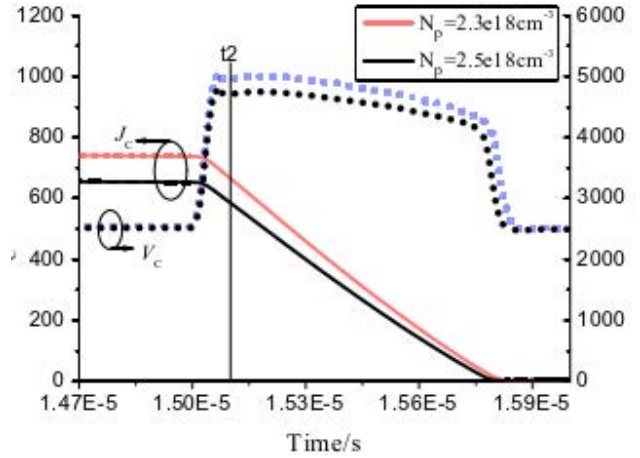


(b) Electric field and hole density distribution diagram at time t1

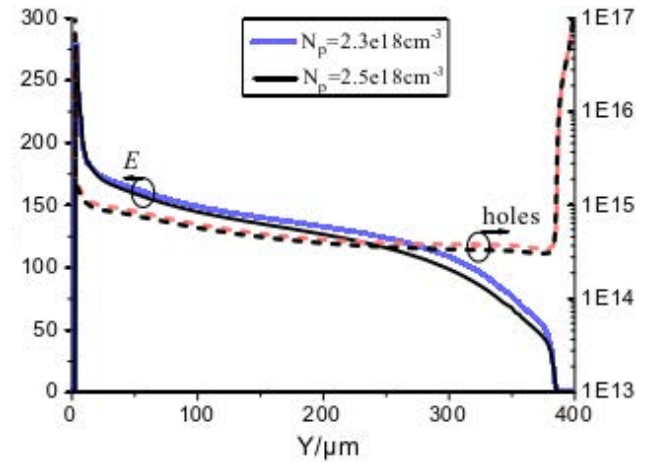
**Figure 11 Short-circuit current, voltage curves and electric field and hole density distribution diagram at time t1 under different p-base region concentrations**

Figure 12 is the electric field intensity curve at time t2 when  $x=28$  microns at time t2, in the short-time II mode, under different p-base region densities. It can be seen from the chart that when  $N_p$  is low, its short-circuit current density, induced voltage peak and dynamic collapse duration will increase.  $E_p$  is  $2.3 \times 10^5$  V/cm at t2, and its value is  $2.8 \times 10^5$  V/cm, which is slightly larger than  $E_p$ 's  $2.5 \times 10^{18}$  cm<sup>-3</sup>. When  $N_p$  is low, the dynamic avalanche phenomenon during short-circuit II turn-off will also be intensified[8]. Therefore, increasing the concentration of the p-base region is beneficial to improving the kinetic av-

alanche performance of the short-circuit type II reaction.



(a) Short circuit II turn-off current and voltage curves



(b) Electric field and hole density distribution diagram at time t2

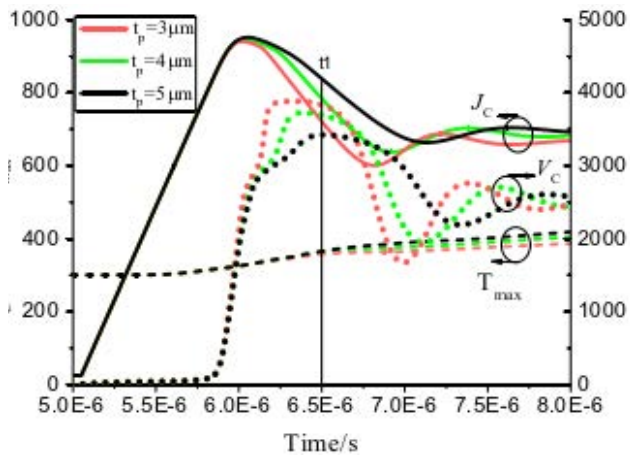
**Figure 12 Short-circuit II turn-off current, voltage curve and electric field and hole density distribution at time t2 under different p-base region concentrations**

### 2.3 Collector area thickness

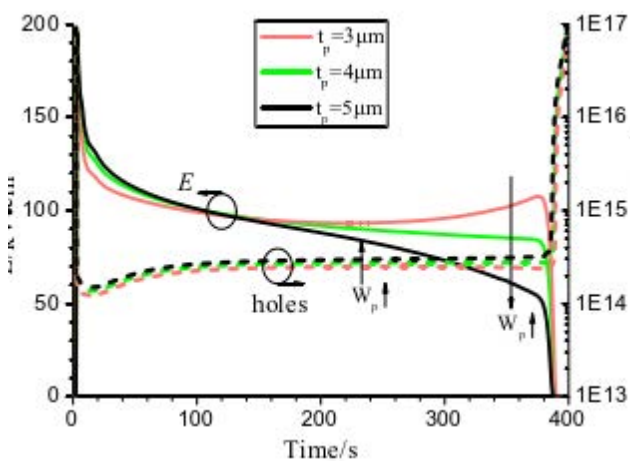
The thickness of the collector region has a greater impact on its short-circuit performance than the thickness of the nanoribbon. Therefore, this article only discusses the thickness effect of the collector area. Figure 13 (a) is the voltage, current and maximum junction temperature curves during short circuit in the on state, and the longitudinal section of the maximum field strength at t1 and the corresponding hole concentration section are shown in Figure 13 (b). The collector injection efficiency increases with the thickness of the collector region, so more holes are injected in the collector region, resulting in increased effective charge density, steeper electric field gradients, and larger  $E_p$ . Therefore, when a short circuit occurs

and the voltage rises, at the same voltage, as the collector injection efficiency increases,  $E_{pn}$  also increases. Therefore, the 5-micron (5-micron) structure first experiences a kinetic avalanche, The generation of snow carriers (Snow) will cause the current to decay slowly, the short-circuit voltage to rise more slowly, lower voltage growth, longer avalanche duration and higher temperature[9]. Figure 4-14 shows the local field distribution at  $t_1$ . It can be seen from this figure that as  $t_p$  increases,  $E_{pn}$  also increases.  $E_{pn}$  is  $1.96 \times 10^5$  V/cm,  $t_p$  is 5 microns.

The greater the base thickness of the IGBT collector area (the higher the collector injection efficiency), the greater the peak electric field of the pn junction under short-circuit current, the more severe the dynamic collapse, the longer the maintenance time, the higher the temperature, and the easier it is to fail under short-circuit conditions. .



(a) Current and voltage curves when short circuit II occurs



(b) Electric field and hole density distribution diagram at time  $t_1$

**Figure 13 Short-circuit II turn-on current, voltage curves and electric field and hole density distribution at time  $t_1$  under different  $t_p$**

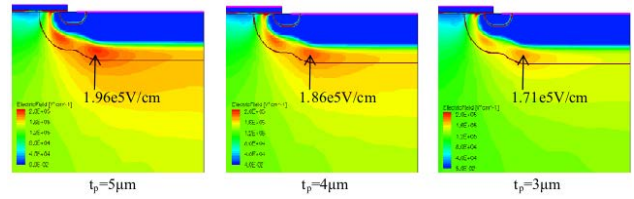
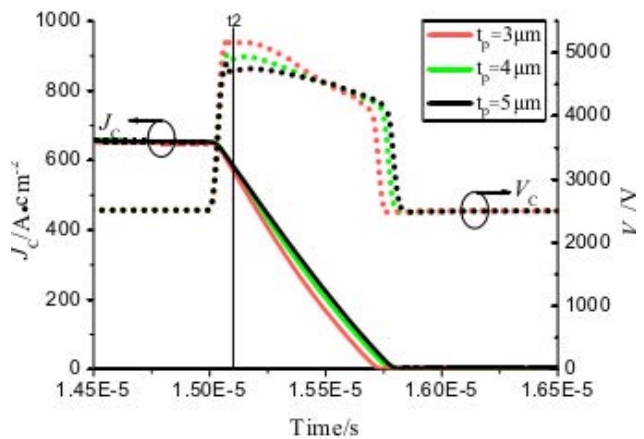
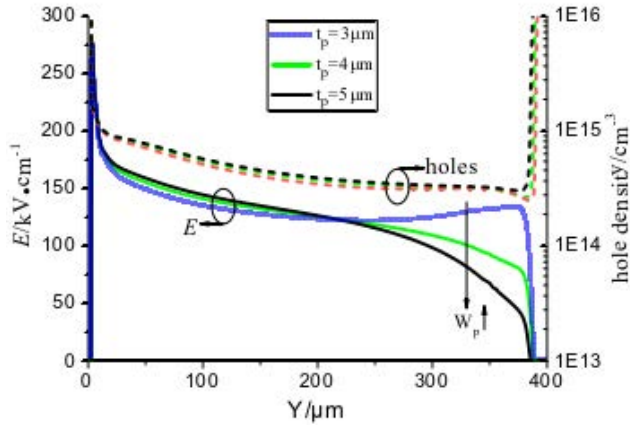


**Figure 14 Local electric field distribution diagram of different  $t_p$  at time  $t_1$**

Figure 15 shows the field intensity distribution at  $x=28$  microns at  $t_2$  under different p-base region concentrations in the second short-circuit mode. As shown in the figure, as the thickness of the p-type current collection region increases, the induced voltage peak decreases, but the dynamic avalanche duration increases. As shown in Figure 15 B, when  $t_p$  is larger, more holes are injected into the collector area, and the electric field becomes steeper,  $E_{pn}$  is the same, but the difference is very small. However, as the collapse time increases, the voltage and current decrease slowly, which means that the increase in holes causes the J2 junction electric field to decrease more slowly, and the dynamic collapse lasts longer. Therefore, as the thickness of the p-type current collector increases, the dynamic avalanche effect generated during the second short-circuit turn-off process will also increase. Therefore, reducing the thickness of the p-type collector region is beneficial to improving the dynamic avalanche performance of the type II short-circuit process.



(a) Short circuit II turn-off current and voltage curves

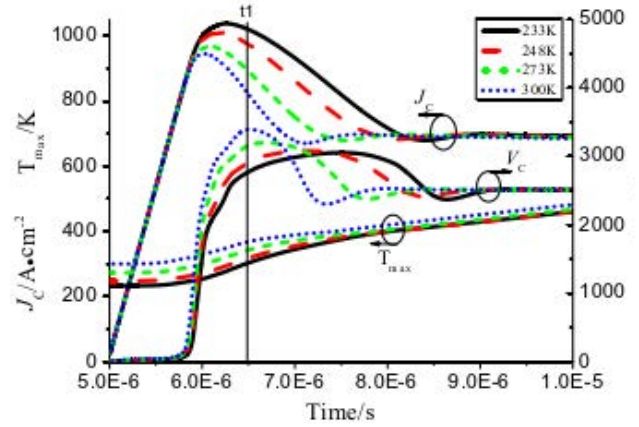


(b) Electric field and hole density distribution diagram at time t2

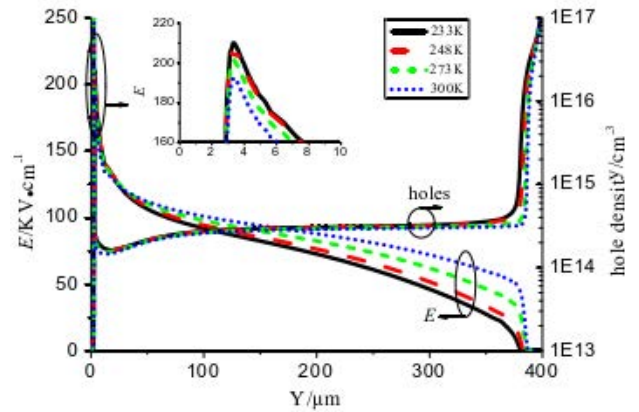
**Figure 15 Short-circuit II turn-off current, voltage curve and electric field and hole density distribution at time t2 under different  $W_p$**

### 3 Effect of low temperature on dynamic avalanche during short circuit

Figure 16 (a) is the voltage, current and maximum junction temperature curves when a short circuit occurs in short circuit II mode. It shows that the increase in short circuit voltage decreases with the decrease of temperature, and as the dynamic avalanche prolongs, the amplitude of increase increases. It also increased accordingly[10]. Figure 16 (b) is the longitudinal electric field and hole concentration distribution diagram under the maximum field strength of t1. At low temperature, the drift rate of carriers is lower, so compared with room temperature, the plasma interface is closer to the emission region; At low temperatures, the electric field broadens more slowly, and the electric field width is closer to the emission region. At t1, at lower temperatures, higher temperatures and more holes are injected, causing  $E_p n$  to reach  $2.1 \times 10^5$  V/cm and  $1.92 \times 10^5$  V/cm at 233 K and room temperature, respectively. In addition, under low temperature conditions, the avalanche impact ionization rate is higher, making it easier to generate dynamic avalanches under low pressure conditions, and the longer the avalanche duration, the higher the temperature. Therefore, the ability to withstand dynamic avalanches at low temperatures is poor under on-state short circuit conditions.



(a) Current and voltage curves when short circuit II occurs

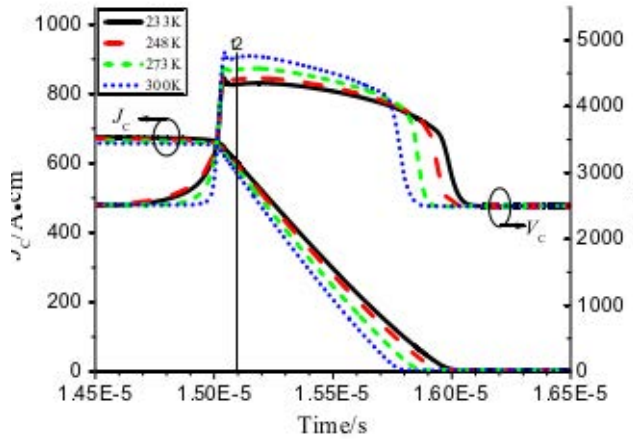


(b) Electric field and hole density distribution diagram at time t1

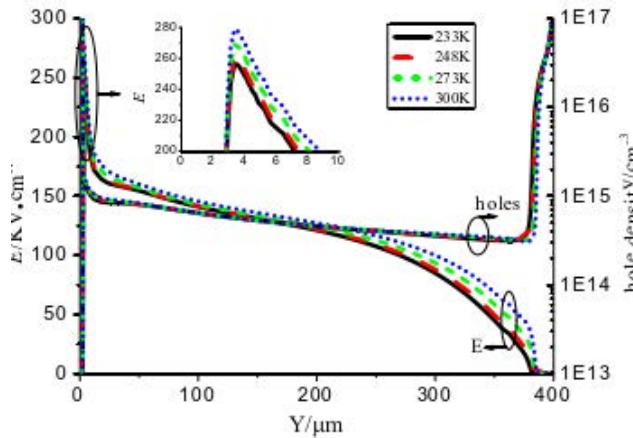
**Figure 16 Current and voltage curves and electric field and hole density distribution diagram at time t1 when short circuit II occurs at normal and low temperatures**

Figure 17 shows the field strength distribution and carrier concentration distribution at time t2 at  $x=28$  microns at normal temperature. It can be seen from the chart that at lower temperatures, the short-circuit turn-off voltage is lower and the avalanche duration is longer. As shown in Figure 17 B, at lower temperatures, the plasma is closer to the emitter electrode side, and the electric field is compressed more to the emitter region side. This is due to the higher avalanche-impact ionization rate at low temperatures, which lowers the clamping voltage, reduces carrier extraction and prolongs the avalanche duration. Therefore, under low temperature conditions, high collision ionization rates cause dynamic avalanches to proceed at lower voltages, and dynamic avalanches last longer, so the ability to resist dynamic avalanches under low temperature conditions is relatively weak.





(a) Current and voltage curves when short circuit II is turned off



(b) Electric field and hole density distribution diagram at time t2

**Figure 17 Short circuit II turn-off current, voltage curve and electric field and hole density distribution at time t2 at normal and low temperatures**

## Conclusion

This paper conducts research on the generation mechanism and influencing factors of dynamic collapse under type II short circuit conditions. Research has found that during type II short circuit, the regulation of the electric field by carriers causes a dynamic avalanche in the J2 junction under low voltage, and under strong dynamic collapse conditions, the holes formed by the avalanche are more likely to form latches through the p-base region. Under large sensitivity, when the short-circuit current is turned off, because the induced voltage is too high, dynamic collapse will occur at the J2 junction, resulting in clamping, causing the coil temperature to rise, and even causing the device to burn out.

Through a comparative study of the dynamic avalanche characteristics of the two structures in the type II short-circuit state, it was found that increasing the cell size, increasing the p-base concentration and reducing the injection efficiency of the collector can effectively improve the short-circuit process. Dynamic avalanche properties. The study found that the dynamic avalanche effect is more significant in short-circuit II mode and low temperature conditions, which can produce a larger voltage clamp under lower voltage conditions and maintain it for a longer time.

## References

- [1] Ma Yao, Xu Lipin, Yu Wei, Liu Min'an & Ren Yadong. (2023). Research on energy conduction and energy impact of IGBT failure. *Locomotive Electric Transmission* (05), 162-169.
- [2] Zhang Lantao, Xiong Jun, Niu Xiaonan & Huang Xiaoyu. (2022). The impact of uneven current flow at parallel power ports on the thermal characteristics of IGBT modules. *Electrical Drives* (09), 46-49+80.doi:10.19457/j. 1001-2095.dqcd22609.
- [3] Zhang Yanxia, Du Shanshan, Ma Jinting & Dong Guanghao. (2023). Research on IGBT valve protection scheme in VSC-HVDC system. *Journal of Electrical Machines and Control* (12), 31-40.
- [4] Su Rongjie, Du Mingxing & Li Bao. (2023). An IGBT module bonding wire aging monitoring method based on short-circuit current. *Computer Applications and Software* (05), 76-82.
- [5] Du Jiguang, Ding Xinnan & Wang Weizheng. (2023). Application of IGBT short-circuit protection strategy based on digital control. *Electronic Technology* (04), 40-41.
- [6] Gao Dongyue, Ye Fengye, Zhang Dahua, Luo Jian & Gao Jinwen. (2022). 3300 V IGBT module with low leakage and strong short circuit capability. *Solid Electronics Research and Progress* (02), 81-85+98.
- [7] Zhang Tian, Song Mingxuan, Feng Yuan & He Fenyong. (2022). Research on the series short-circuit dynamic characteristics of SiC MOSFET and Si IGBT. *Electrical Transmission* (21), 3-7.
- [8] Wu Yilin, Yang Yixuan, Zhang Sheng, Gao Chong, He Zhiyuan & Tang Guangfu. (2023). Design and implementation of MMC sub-module IGBT short circuit experimental platform. *Chinese Journal of Electrical Engineering* (16), 6384-6395.
- [9] Zhou Donghai, Zhang Dahua, Ye Fengye, Gao Dongyue & Chao Wujie. (2022). Research on short-circuit hot spots and performance improvement of high-voltage IGBT. *Semiconductor Technology* (03), 192-198.
- [10] Li Hui, Yu Yue, Yao Ran, Lai Wei, Xiang Xuefeng & Li Jinyuan. (2023). Analysis of short-circuit failure mechanism of press-fit IGBT devices based on multi-level simulation. *Chinese Journal of Electrical Engineering* (06), 2392-2404 .

Acknowledgments

Time passed quickly, and in the blink of an eye, my journey to study came to an end. In the future, I will switch from the role of a student to a new job and start a new life journey. Recalling the scenes during my study period, there is the joy of success, the frustration of failure, the hardship of struggle, and the satisfaction of harvest. Some of them can still clearly appear in front of my eyes. They will be An indispensable part of my life memory. First of all, I would like to express my gratitude to my super-

visor. Under his guidance, my thesis can be successfully completed. Secondly, I would like to thank my parents. They always give me encouragement and support when I encounter difficulties and setbacks, allowing me to have a relaxed and comfortable family environment. Finally, I would like to thank everyone who participated in my Thank you to all the anonymous reviewers and reviewers for my defense for your suggestions, which made my thesis more perfect and reasonable.